Papers

Diffusive component of the vertical flux of particulate organic carbon in the north polar Atlantic*

MAŁGORZATA STRAMSKA

Center for Hydro-Optics & Remote Sensing (CHORS),
San Diego State University,
6505 Alvarado Rd., Ste. 206, San Diego, CA 92120, USA;

e-mail: mstramska@ucsd.edu

Abstract

The diffusive component of the vertical flux of particulate organic carbon (POC) from the surface ocean layer has been estimated using a combination of the mixed layer model and ocean color data from the SeaWiFS satellite. The calculations were carried out for an example location in the north polar Atlantic centered at 75°N and 0°E for the time period of 1998–2004. The satellite estimates of surface POC derived using a regional ocean color algorithm were applied as an input to the model driven by local surface heat and momentum fluxes. For each year of the examined period, the diffusive POC flux was estimated at 200-m depth from April through December. The highest flux is generally observed in the late fall as a result of increased heat loss and convectional mixing of surface waters. A relatively high diffusive POC flux is also observed in early spring, when surface waters are weakly stratified. In addition, the model results demonstrate significant interannual variability. The highest diffusive POC flux occurred in 1999 (about 4500 mg m^{-2} over the 9-month period). In 1998 and 2002 the estimated flux was about two orders of magnitude lower. The interannual variability of the diffusive POC flux is associated with mixed layer dynamics and underscores the importance of atmospheric forcing for POC export from the surface layer to the ocean's interior.

The complete text of the paper is available at http://www.iopan.gda.pl/oceanologia/

1. Introduction

The availability of solar energy and nutrients in surface oceanic waters enables fixation of inorganic carbon into organic matter during the process of photosynthesis in phytoplankton. The fixation of inorganic carbon into organic matter in the photic zone, its transformation by foodweb processes, and subsequent vertical transport by physical mixing and gravitational settling of particles, are commonly called the biological pump (e.g., Ducklow et al. 2001). Because of the potential impact on the atmospheric CO_2 budget and global climate, determining the strength of the biological pump, including the magnitude of the fraction of primary production (PP) that is removed from the euphotic zone (export production (EP), e.g., Dugdale & Goering 1967, Eppley & Peterson 1979, Eppley 1989) has been a high priority research goal in oceanography.

Several approaches have been developed to estimate the fraction of primary production that is transported from surface waters to greater depths. The experimental approaches include direct measurement of vertical particulate fluxes with moored or drifting sediment traps (e.g., Martin et al. 1993; see also reviews by Antia et al. 2001, Berelson 2001 and Lutz et al. 2002) and application of naturally occurring radionuclides, for example, thorium-234 (^{234}Th), as tracers for sinking particles (e.g., Buesseler et al. 1992, 1995). The modeling approaches for estimating the strength of the biological pump include food web and particle transformation models (e.g., Boyd & Stevens 2002, Legendre & Rivkin 2002), ecosystem models (e.g., Pätsch et al. 2002, Lima & Doney 2004), and inverse models of biogeochemical processes based on regional distributions of oxygen, dissolved nutrients, and carbon in the ocean (Anderson et al. 2000, Schlitzer 2002, 2004, Schlitzer et al. 2003, Usbeck et al. 2003). Approaches in which primary and export production are estimated from chlorophyll distributions obtained from ocean color satellite data have also been developed (e.g., Antoine et al. 1996, Behrenfeld & Falkowski 1997, Laws et al. 2000, Behrenfeld et al. 2005). In contrast to in situ measurements, which are usually limited geographically and temporally, satellite and modeling methods have the advantage of providing export estimates for extended periods of time for large regional, basin, and global scales. Unfortunately, all present POC flux estimates involve considerable uncertainties for a variety of reasons. For example, satellite estimates of export production rely on the assumed conversion of chlorophyll a (Chl) to productivity rates, phytoplankton Chl/POC ratios, and f ratios (i.e., EP/PP ratios), which are difficult to quantify accurately or verify with a limited number of in situ calibration sites. A number of issues relating to sediment trap efficiency remain unresolved (e.g., Siegel & Deuser 1997). Inverse model calculations

suggest higher estimates of POC fluxes from surface to mid-water depths than the sediment trap and satellite-based methods (Schlitzer 2002, Usbeck et al. 2003). The uncertainties inherent in the current POC flux estimates indicate a need for further development of alternative ways for studying POC dynamics in the ocean.

A new approach for investigating POC dynamics and fluxes in the ocean, which combines the mixed layer model and satellite observations of ocean color, is presented in this paper. The surface POC concentrations are first determined from satellite imagery. These estimates are then used as input to a physical mixed layer model, which allows us to investigate the effects of physical forcing on POC dynamics and export from the ocean surface layer, assumed in our study as the top 200-m layer. This method requires no assumptions about the relationship between Chl and PP or Chl and POC as it is based on a direct assessment of POC concentration from ocean color. As a starting point, a relatively simple version of the physical model (a one-dimensional mixed layer model) was used for the calculations. This paper demonstrates significant seasonal and interannual variability in the diffusive component of the POC flux in response to atmospheric forcing at an example location in the north polar Atlantic. The estimated diffusive POC flux is due to local mixing, represents a fraction of the total POC export, and can be regarded as the lower limit of the total POC export.

2. Material and methods

Meteorological and surface POC data were used as surface boundary conditions for the mixed layer (ML) model, as described below. Although the results are presented for one example location in the north polar Atlantic centered at 75°N and 0°E, our methodology is general and applicable to other geographical locations. For the purpose of revealing seasonal and interannual variability in the diffusive POC flux, the model calculations were made for the months of April through December over several years from 1998 to 2004. The principal reasons for omitting the months of January–March from our analysis is the lack of sea ice processes in our physical model and the lack of satellite ocean color data during that part of the year because of the polar night.

2.1. Model

For simulations of the temporal evolution of the vertical distribution of POC in the surface layer of the ocean and the vertical flux of POC out of the surface layer, the one-dimensional (1D) version of the level 2.5 Mellor-Yamada (MY) mixed layer model was used (Mellor & Yamada 1974, 1982,

Blumberg & Mellor 1983; see also Mellor 2004). This model belongs to the class of differential ML models. In contrast to integrated ML models, the MY model enables the computation of vertical profiles of turbulent variables and includes realistic, stability-dependent eddy diffusivity coefficients. These features of the model are important for examining the relationships between local atmospheric forcing and POC dynamics in surface waters.

We recall only a few basic equations of the MY model (see Mellor 2004 for details). The model solves the turbulent forms of the momentum and thermodynamic equations with some simplifying assumptions for closing the system. For a horizontally homogenous ocean with no mean vertical water motion, the equations of conservation of momentum and heat can be written as follows:

$$\frac{\partial U}{\partial t} - f(V - V_g) = \frac{\partial}{\partial z}\left[(K_M + \nu_M)\frac{\partial U}{\partial z}\right] \tag{1}$$

$$\frac{\partial V}{\partial t} - f(U - U_g) = \frac{\partial}{\partial z}\left[(K_M + \nu_M)\frac{\partial V}{\partial z}\right]$$

$$\frac{\partial T}{\partial t} = \frac{\partial}{\partial z}\left[(K_H + \nu_H)\frac{\partial T}{\partial z}\right] + \frac{1}{\rho_0 c_p}\frac{\partial I}{\partial z},$$

where t is time, z the vertical coordinate, U and V the mean horizontal velocity components, T the mean water temperature, I the irradiance, f the Coriolis parameter, K_M and K_H the eddy coefficients for vertical turbulent diffusion, ν_M and ν_H the coefficients for molecular and background diffusion, ρ_o the water density, and c_p the specific heat of water. For simplicity, the geostrophic current components U_g and V_g were taken to be zero. The equation set (1) is closed using the following formulas for the eddy coefficients:

$$K_M = l\,q\,S_M \tag{2}$$
$$K_H = l\,q\,S_H,$$

where l is the turbulent length scale, $q^2/2$ the turbulent kinetic energy, and S_M and S_H are stability functions dependent on the local Richardson number. The temporal evolution of the vertical profiles of POC concentration was described by adding the following equation to set (1):

$$\frac{\partial \text{POC}}{\partial t} = \frac{\partial}{\partial z}\left[(K_H + \nu_H)\frac{\partial \text{POC}}{\partial z} - (w\,\text{POC})\right], \tag{3}$$

where w is the particle gravitational settling velocity. This description of POC dynamics is based on the following assumptions. Firstly, POC

particles do not affect hydrodynamic processes within the mixed layer. Secondly, the same diffusivity as for other scalar quantities such as salinity and heat also applies to POC. This assumption is at present necessary as no information is available about the diffusivity coefficient for POC in the ocean. Note that similar assumptions are commonly used in models simulating phytoplankton dynamics in the ocean (e.g., Fasham et al. 1990, Marra & Ho 1993, Druet & Zielinski 1994, Druet 2003, Dzierzbicka-Głowacka 2005a,b). Finally, a constant particle gravitational settling velocity w equal to 2 m day^{-1} is assumed in the calculations. At present there is a significant uncertainty regarding the exact particle sinking velocities within the mixed layer, but a value of about 2 m day^{-1} is often assumed in ecosystem models (e.g., Huisman et al. 1999). To investigate the sensitivity of the model to the uncertainties in w, additional calculations with $w = 0$ and 4 m day^{-1} were also carried out.

For the numerical calculations, eqs. (1) and (3) were transformed into finite difference equations. Because we are interested in the diffusive POC flux out of the surface layer (defined here as the top 200-m layer of the ocean), the vertical grid spacing has been optimized to obtain high vertical resolution of the POC concentration near the surface. The distance between computational grid points increased with depth according to a geometrical progression. The interval was 0.04 m at the surface and there were 400 levels down to a depth of 1405.3 m. The time step was set to 1 minute. The diffusive component of the POC flux discussed in this paper is taken to be the first term in the brackets on the right hand side of eq. (3) and is interpreted as that portion of the total POC export due to mixed layer dynamics.

2.2. Meteorological forcing

The meteorological data from the NOAA-CIRES Climate Diagnostic Center NCEP/NCAR (National Centers for Environmental Prediction and National Center for Atmospheric Research) Reanalysis Project were applied to parameterize the atmospheric forcing used to run the mixed layer model. The Reanalysis Project employs a state-of-the-art analysis/forecast system to assimilate global meteorological data from various available sources from 1948 to the present. In particular, the 6-hour averaged zonal and meridional wind stress components, the net latent, net long-wave, and sensible heat fluxes, as well as the net short-wave radiation flux estimates were used. These data were obtained for the location at 75°N and 0°E in 1998–2004. In our model the net heat loss calculated as the sum of the net latent, net long-wave, and sensible heat fluxes, was applied at the sea surface. The short-wave radiation flux was assumed to penetrate into the water column

and to act as the internal heat source. The absorption of solar radiation was calculated according to Paulson & Simpson (1977) for class I waters, corresponding to open ocean waters (Jerlov 1968).

To summarize the seasonal and interannual variability of atmospheric forcing, Fig. 1 displays the total net heat flux calculated as the sum of all the composite heat fluxes including short-wave radiation. Fig. 2 presents the
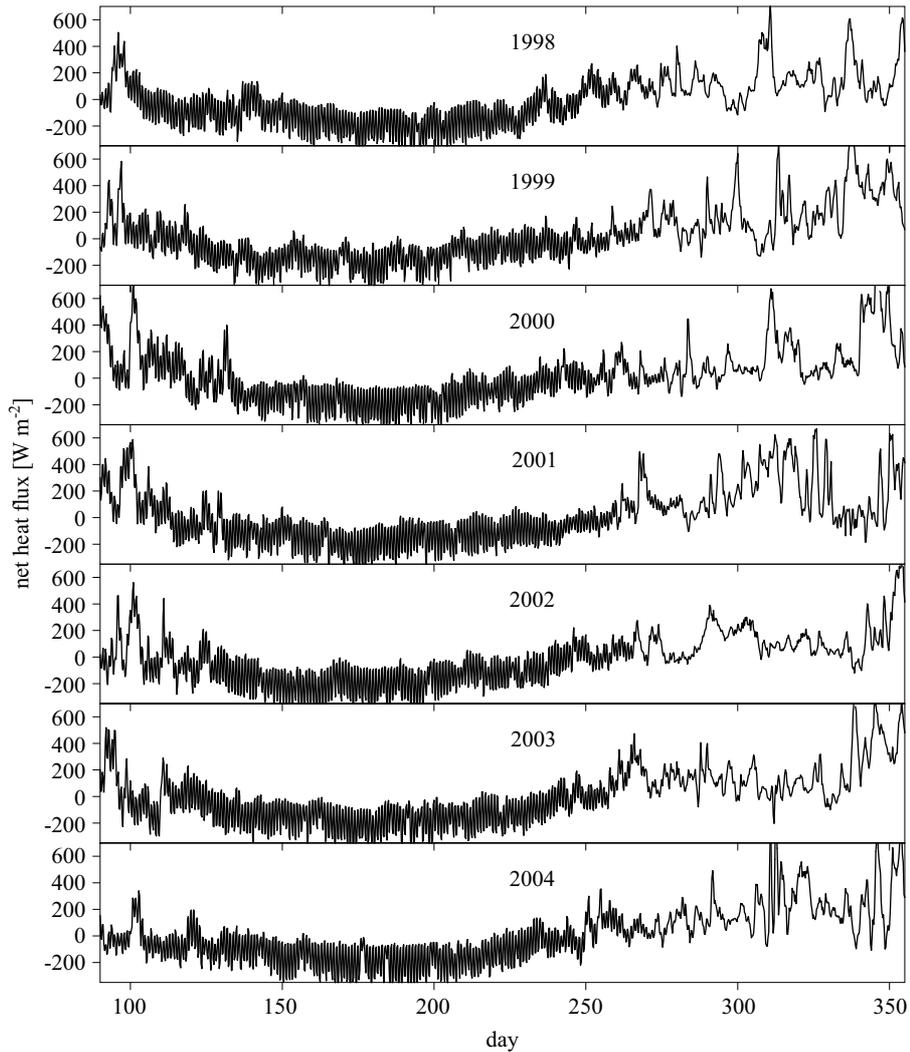
Fig. 1. Net heat flux time series at 75°N and 0°E derived from the data from the NOAA-CIRES Climate Diagnostic Center NCEP/NCAR (National Centers for Environmental Prediction and National Center for Atmospheric Research) Reanalysis Project
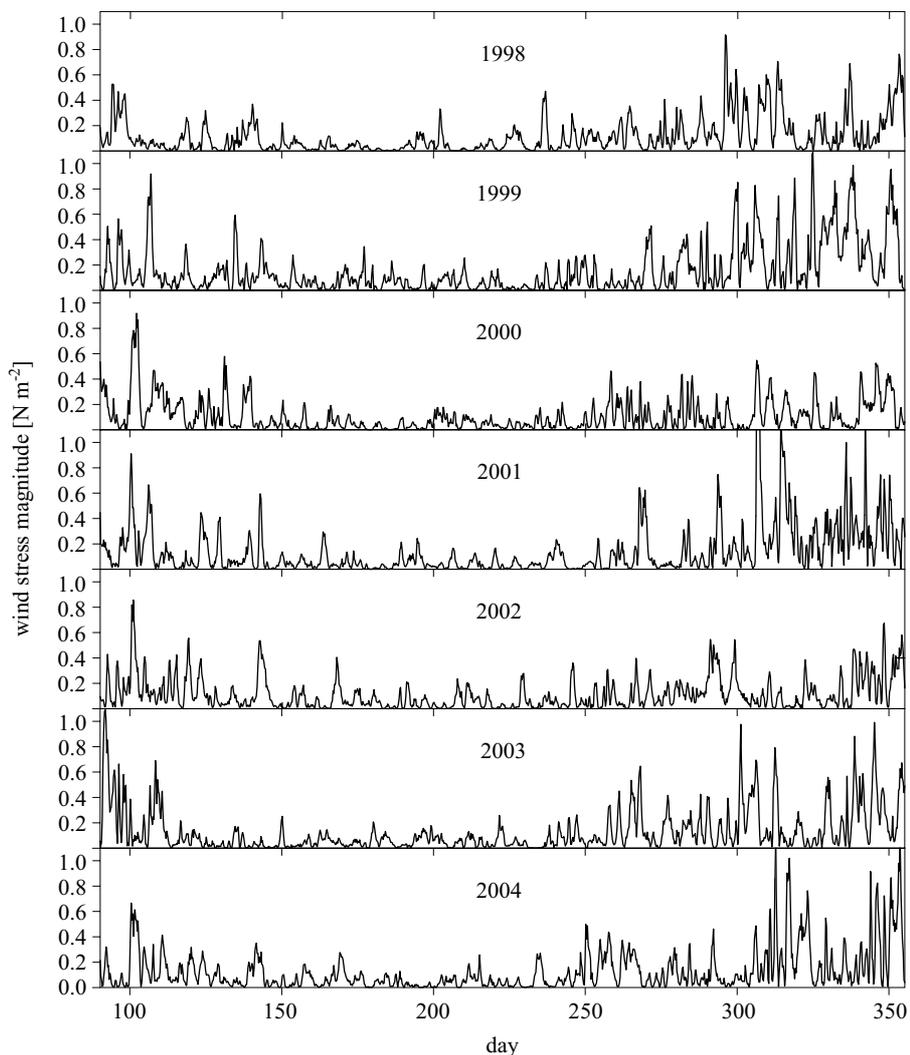
Fig. 2. Time series of wind stress magnitude at 75°N and 0°E derived from the data from the NOAA-CIRES Climate Diagnostic Center NCEP/NCAR (National Centers for Environmental Prediction and National Center for Atmospheric Research) Reanalysis Project

magnitude of wind stress calculated as the square root of the sum of squared zonal and meridional wind stress components. Note that for simplicity our version of the model assumes a null salinity flux at the ocean surface, i.e., the model does not account for changes in water salinity due to sea ice processes, evaporation, and precipitation. The latent heat of evaporation is included in the calculations of the net heat flux.

2.3. Model initialization and boundary conditions

The model run started on day 81 and ended on day 365 for each year examined. The model was not run on days 1–81, because our version of the model did not take sea ice processes into consideration. The first 10 days of the run (i.e., end of March) were used for model spin-up and are not discussed here. The results presented are for the months of April through December.

The initial profiles of water temperature, salinity and POC concentration used to start the calculations were assumed to be the same for all the years. Initial POC was taken to be homogenous throughout the water column and equal to 10 mg m^{-3}. Initial temperature and salinity profiles are shown in Fig. 3. These profiles were measured on March 17, 1989 at 75.5°N and 0.5°W during the Greenland Sea Project. The data were made available through the PANGAEA data base (see also GSP/AOSB/ICES 2002, Compiled data set of 1589 oceanographic stations of the Greenland Sea Project, PANGAEA doi:10.1594/PANGAEA.84534; GSP/AOSB/ICES (1993), Greenland Sea Project, International Council for the Exploration of the Sea (ICES), Oceanographic database and services, http://www.ices.dk/ocean/project/data/gsp.htm).
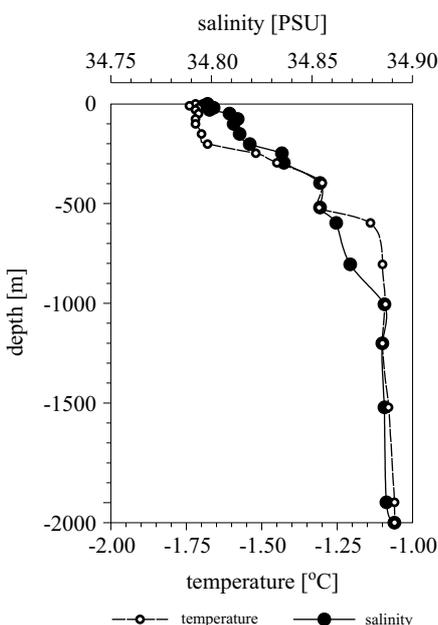
Fig. 3. Initial water temperature and salinity profiles used for the mixed layer model. These data were measured on March 17, 1989 at 75.5°N and 0.5°W as a part of the Greenland Sea Project (http://www.ices.dk/ocean/project/data/gsp.htm)

Water temperature, salinity, and POC concentration were assumed to be constant at the bottom depth. On the basis of the Greenland Sea Project data set it was confirmed that this assumption is reasonable for

water temperature and salinity. No data on deep-water POC concentration from the Greenland Sea region were found. The Bermuda Atlantic Time Series (BATS) site (31.6°N, 64.2°W) is the nearest location where time series of deep-water POC concentration are available. At BATS the POC concentrations close to the assumed value of 10 mg m^{-3} were observed at 1000 m depth in 2000–2002 (see http://bats.bbsr.edu).

2.4. Surface POC concentrations

Time series data of the surface POC concentration were derived from satellite ocean color imagery collected with the SeaWiFS instrument (e.g., Hooker & McClain 2000) over a period of 7 years from 1998 through 2004. The SeaWiFS provides global coverage of normalized water-leaving radiance L_{wn} at eight spectral bands in the visible and near-infrared spectral region approximately every two days. The standard NASA data processing procedures used to derive L_{wn} involve atmospheric corrections and removal of pixels with land, ice, clouds, heavy aerosol load, or negative values of retrieved radiances (e.g., Gordon & Wang 1994). Our analysis is based on Level 3 standard mapped images (SMI), which are projections of the Global-Area-Coverage data onto a global, equal-angle grid with a nominal 9 km × 9 km resolution (reprocessing version 4). One-day composites of L_{wn} were selected for our analysis. These data were obtained from the Goddard Earth Sciences Data and Information Services Center, DAAC (at present the NASA Ocean Color Web Site).

From L_{wn}, the POC concentrations were estimated using the two-step empirical algorithm derived for the north polar Atlantic region (Stramska & Stramski 2005). This algorithm operates in such a way that the particulate beam attenuation coefficient at 660 nm, $c_p(660)$, is estimated first from the satellite-derived blue-to-green ratio of normalized water-leaving radiances, $L_{wn}(443)/L_{wn}(555)$. Next, the POC vs. $c_p(660)$ relationship is used to calculate the surface POC concentration:

$$c_p(660) = 1.0976\,e^{-0.7542R} \quad \text{where} \quad R = L_{wn}(443)/L_{wn}(555), \qquad (4)$$

$$\text{POC} = 554.82\,c_p(660)^{1.3093}, \qquad (5)$$

where POC is in [mg m^{-3}], c_p is in [m^{-1}] and L_{wn} is in [μW cm^{-2} nm^{-1} sr^{-1}]. The satellite-derived POC concentrations estimated with relationships (4) and (5) were subsequently binned within a 1° × 1° cell (i.e., the area from 74.5°N to 75.5°N and from 0.5°W to 0.5°E) to filter out smaller scale variability. For the days when there were less than 15 pixels with valid satellite data within the cell (out of ∼100 pixels in the cell), we assumed that the POC concentration could not be estimated from $L_{wn}(443)/L_{wn}(555)$

with a sufficient level of confidence. In these cases the daily POC concentration was assumed to be equal to the concentration obtained from linear interpolation of the closest available days.

The local heat and momentum fluxes and surface POC data for the years 1998–2004 were used to run the MY model. The original heat fluxes and wind stress data were interpolated linearly to provide one-minute temporal resolution data appropriate to the time step used in the model. Similarly, the surface POC data from April through September were interpolated with
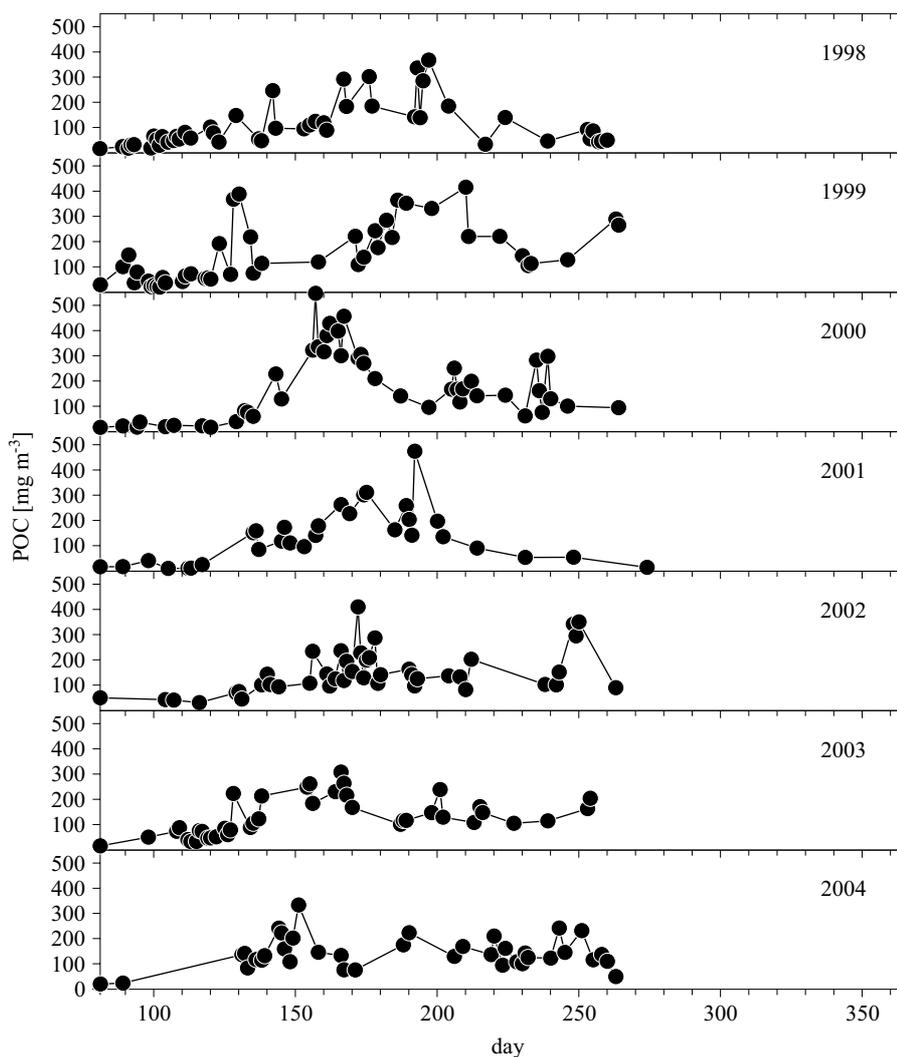
Fig. 4. Time series of surface POC concentration at 75°N and 0°E estimated from SeaWiFS ocean color data (see eqs. (3) and (5))

the same time resolution until the last daily POC data available in the year (usually at the end of September). Later in the year, no satellite ocean color data are available for the examined location (frequent clouds, polar night, sea ice). Therefore, for that remaining part of the year, the surface POC concentration was adjusted within the model, assuming that POC sources within the mixed layer are equal to zero.

Fig. 4 shows satellite-derived surface POC concentrations estimated with the described method (eqs. (4) and (5)). This plot illustrates the fact that our site in the north polar Atlantic region is characterized by a wide seasonal range of POC concentrations, with higher values occurring from May through the summer and lower values in early spring and late fall. The lowest POC concentrations of the season are observed in April. The POC concentrations in May are significantly higher than in April and can exceed 300 mg m^{-3}. In June and July the POC values may also be as high. With further progression of the season, POC generally starts to decline in late August. It is also important to note that the overall pattern of interannual variability of POC concentration at the study site is quite complex: for example, the yearly maximum POC values were observed in different months over the 7-year period.

3. Results

The application of our model to a 7-year long record of SeaWiFS data reveals patterns of seasonal and interannual variability of the vertical diffusive flux of POC at 75°N and 0°E. Unless otherwise stated, we discuss the diffusive flux at 200 m depth (POC$_{200}$) estimated with model runs using a constant particle gravitational settling velocity, $w = 2$ m day^{-1}. Additional calculations with $w = 0$ and $w = 4$ m day^{-1} yield very similar estimates of the diffusive POC flux at 200-m depth; therefore, the results from these model runs are presented only briefly at the end of this section. Note that to a first approximation, the 200-m depth can be considered the lower limit of the photic zone in our location during the productive season of the year.

Throughout the period when the seasonal phytoplankton bloom develops (in April–May), the estimated POC$_{200}$ values are higher in years when the net heat loss from surface waters to the atmosphere prevents significant thermal stratification of the water column (Fig. 5a). In those years weakly stratified water allows for the development of deep mixing events associated with the passage of storm systems through the north polar Atlantic. Such mixing events are an efficient mechanism for transporting POC particles below the 200 m depth. As a result, the interannual pattern of POC$_{200}$ in April-May closely follows the interannual variability in net heat flux, with the highest POC$_{200}$ values in the year 2000 ($\sim$10 mg m^{-2} day^{-1}). Surface

a
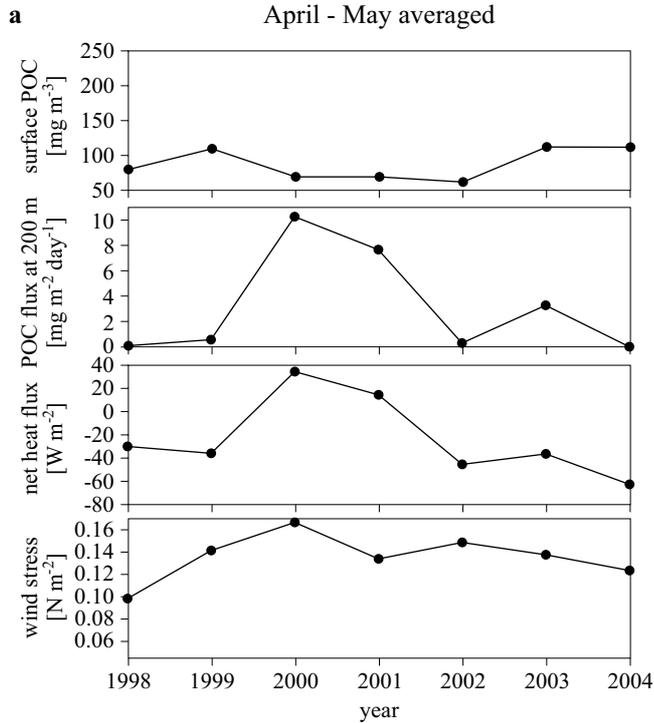
Fig. 5. Estimates of the diffusive POC flux at 200 m at 75°N and 0°E, averaged for the following periods: April–May (a); June–July (b); August–September (c); October–December (d). These estimates were derived from the surface POC concentrations shown in Fig. 4 and the 1D mixed layer model as described in the text. The averaged surface POC concentration, net heat flux (positive for heat loss from the ocean), and the magnitude of the wind stress for each time period are also shown

POC concentrations are considerably higher in summer and early fall than in spring, with average values between 150–240 mg m^{-3} in June–August and between 70–200 mg m^{-3} in September–October (Fig. 4). In contrast to this seasonal trend in POC concentrations, the estimated POC$_{200}$ is significantly lower (1–3 mg m^{-2} day^{-1}) in June–October than in spring, and shows little interannual variability (Fig. 5b and c). A dramatic increase in POC$_{200}$ takes place in late fall, which can be attributed to considerable cooling of surface waters due to the seasonal increase in heat loss accompanied by a larger wind stress magnitude (Fig. 5d). As a consequence, POC$_{200}$ averaged over the November–December time period reaches values as high as 70 mg m^{-2} day^{-1} in 1999. The highest POC$_{200}$ value observed in 1999 corresponds to both the high surface POC concentration and the high turbulent kinetic energy transfer from the atmosphere to the ocean observed

b
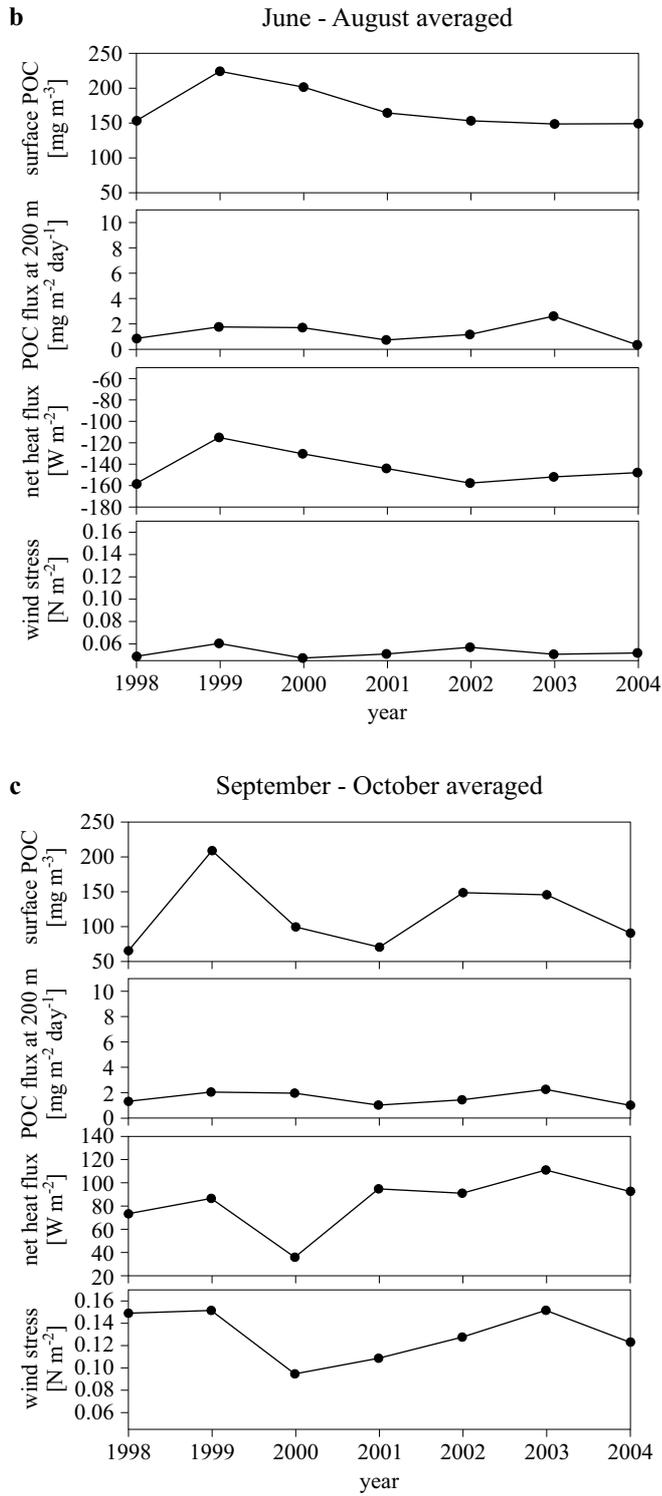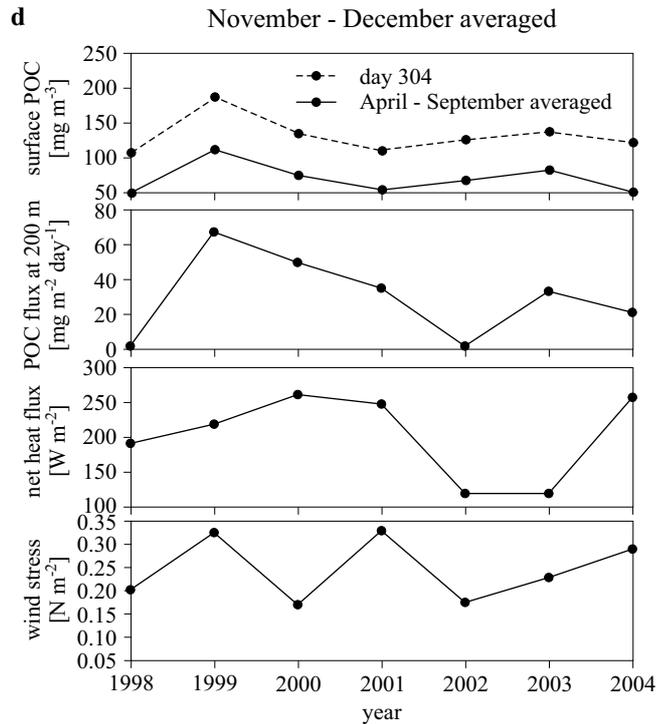
Fig. 5. (*continued*)

Fig. 5. (*continued*)

in the fall (i.e., the substantial net heat loss from the ocean as well as the high wind stress magnitude). Because in the November-December period the estimated POC_{200} considerably exceeds the estimates for other time periods of the year, the interannual pattern of seasonally integrated POC_{200} (Fig. 6) is similar to the POC_{200} pattern for November–December (Fig. 5d). For comparison, Fig. 6 shows values of POC_{200} estimated with w equal to 0, 2, and 4 m day^{-1}, but these estimates are nearly identical, and hence the lines are indistinguishable from one another.

4. Discussion

It is of interest to compare our estimates of the diffusive component of POC flux with the total POC flux assessed from historical sediment trap data from the same region. Unfortunately, however, it seems that there are no sediment trap data from the location examined in our model and in the same time period covered by the SeaWiFS observations. Our comparison is therefore based on two indirect approaches. In the first approach we compare our modeled diffusive component POC_{200} with the total POC flux estimated from a sediment trap deployed at the same location (i.e., 75°N
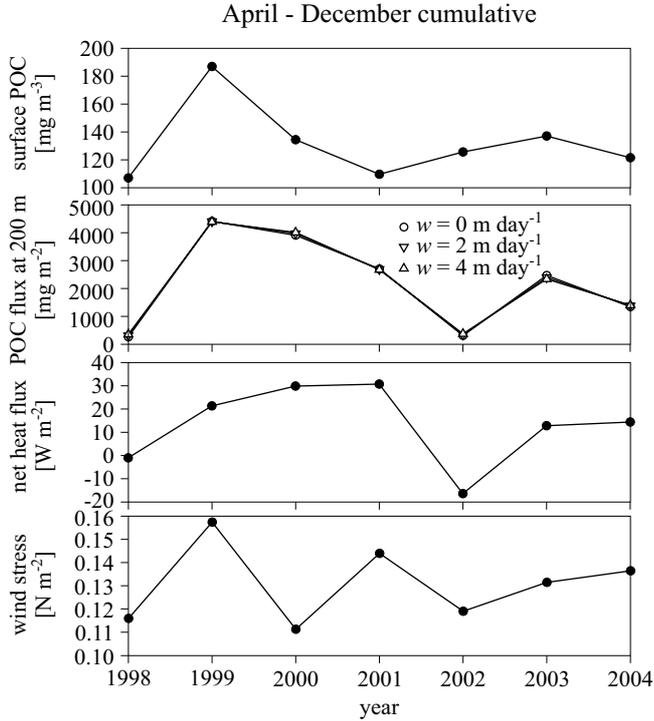
Fig. 6. Estimates of seasonally integrated (April–December) diffusive POC flux at 200 m at 75°N and 0°E in different years. The averaged surface POC, net heat flux (positive for net heat loss from the ocean), and the magnitude of the wind stress are also shown for each year

and 0°E) but not at the same time period. The trap was deployed at 200 m depth from August 1993 through May 1994. It was then recovered and redeployed at 300 m depth till June 1995 (Noji et al. 2000). There was a significant interannual and seasonal variability in POC flux documented by the trap data with a large sedimentation peak observed in the fall of 1994. In the second approach the model-derived POC_{200} is compared with the POC flux measured at 500 m depth with sediment traps deployed at $\sim 72.5°N$ and 7–9.5°W in 1989, 1990 and 1991 (von Bodungen et al. 1995). Assuming that our POC_{200} represents the portion of the total export of POC at 200 m depth, the relationship between POC export (POC_{export}) and POC flux at a given depth z (POC_z) proposed by Martin et al. (1987) was used to calculate the POC_{500}, i.e., the portion of the total flux at 500 m which originates from the diffusive component POC_{200}:

$$POC_z = POC_{export} \left(z/z_o\right)^{-0.858}, \tag{6}$$

where z_o is taken to be 200 m. The Martin et al. relationship accounts for

various processes leading to a transformation of POC flux with depth such as remineralization. This relationship is commonly used in oceanography; for example, it has been adopted by the Ocean Carbon Model Intercomparisons Project as a component of 'standard' biological models (e.g., Lutz et al. 2002).

Table 1 compares our model-based diffusive POC flux with in situ data from sediment traps using these two approaches. These results indicate that the 7-year averaged modeled POC_{200} is within the range of the sediment trap observations of the total POC flux. The POC_{500} estimated using the modeled POC_{200} and eq. (6) is somewhat lower than that derived from the 500 m trap data. This is consistent with our expectation that the total POC flux in the ocean is higher than our model estimates, because POC_{200} accounts only for the diffusive component of the total POC export. Importantly, however, these comparisons indicate that a significant portion of the total POC export from surface waters in the north polar Atlantic is due to mixed layer dynamics, which depends strongly on atmospheric forcing. It is difficult to make a more detailed interpretation of the quantitative differences between the modeled and measured POC fluxes shown in Table 1 because of considerable interannual variability.

Table 1. Comparison of model-derived diffusive POC flux with POC flux data [g m^{-2} $year^{-1}$] from in situ measurements in the north polar Atlantic

Model POC_{200}	POC flux at 500 m estimated from model POC_{200} and eq. (6)	POC flux measured at 200 m at 75°N 0°E	POC flux measured at 500 m at 72.5°N 7–9°W
minimum 0.26	minimum 0.12	-	-
maximum 4.41	maximum 2.01	-	-
average 2.23	average 1.02	1.4–1.92 measured in 1993–1995 (Noji et al. 2000)	3.8; 3.69; 1.07 measured in 1988–1989, 1989–1990, and 1990–1991 respectively (von Bodungen et al. 1995)

The estimates of total POC export can also be derived from primary production (PP) data. Several relationships between the POC flux, PP, and depth have been derived in the past. Antia et al. (2001) compared their estimates of export ratios (i.e., f-ratio) at 125 m with similar empirical ratios derived using the relationships of Betzer et al. (1984), Suess (1980), Pace et al. (1987), and Berger et al. (1987). Differences between these

relationships lead to export ratios at 125 m ranging from 0.12 to 0.39 (see Fig. 5b in Antia et al. 2001). Therefore, it is clear that the choice of the relationship has a major influence on the magnitude of POC flux derived from PP. Nevertheless, the approach of estimating POC fluxes from PP is attractive, because PP is routinely measured on many oceanographic cruises and PP data sets are more extensive than in situ POC export estimates. In addition, improved methods for estimating PP from ocean color satellite data are being developed to enhance spatial and temporal resolution of global PP estimates (e.g., Behrenfeld et al. 2005, Westberry et al. 2006).

In this paper the POC flux was estimated from PP obtained from ocean color data as follows. The SeaWiFS monthly data for May–August in 1998 –2004 for our geographical location were used to calculate the 7-year average PP for that time period from the models of Behrenfeld & Falkowski (1997), Behrenfeld et al. (2005), and Westberry et al. (2006). The PP estimates from these three models are 71.9, 75.0, and 79.1 gC m^{-2} yr^{-1}, respectively (Westberry 2006; private communication). We used these PP estimates to calculate the total POC flux at a given depth z from the relationship of Antia et al. (2001):

$$POC_z = 0.1\, PP^{1.77} z^{-0.68}, \tag{7}$$

where POC_z is the POC flux in [gC m^{-2} yr^{-1}], z the depth in [m], and PP is in [gC m^{-2} yr^{-1}]. This relationship was derived from rigorous analysis of data sets from 27 sites in the North Atlantic covering diverse regions from oligotrophic gyres to subpolar waters (Antia et al. 2001). The total POC flux at 500 m depth estimated from eq. (7) is 2.83, 3.04, 3.34 gC m^{-2} yr^{-1} for the three PP estimates given above. Thus, at our location the 7-year average POC flux at 500 m derived using ocean color-based PP estimates and eq. (7) lies within the range of POC flux from 500 m sediment trap data from earlier years and is somewhat higher than the 7-year average diffusive POC flux estimated from our model and eq. (6) (see Table 1). These results are again consistent with the expectation that our model provides an approximate lower limit of the total POC export flux.

Naturally, the above comparisons have some limitations. It is very difficult to estimate the errors inherent in the estimates compared in this paper. For example, even if some empirical studies suggest approximate relationships for linking primary production and POC flux (e.g., Antia et al. 2001) or POC export and POC flux (e.g., Martin et al. 1987), little is known about possible temporal and regional variability in such relationships (see Lutz et al. 2002 for discussion). The errors in the estimates of POC_{200} derived in this study arise from two main sources. On the one hand, errors are associated with the assessment of the surface POC concentration from

the satellite ocean color algorithm. Up to now, the accuracy of the POC algorithm (eqs. (4) and (5)) has been evaluated with only a limited number of coincident satellite-derived and in situ POC data from the north polar Atlantic. The mean normalized bias (MNB) and the normalized root mean square (RMS) error for this match-up data set were MNB $= -12\%$ and RMS $= 15.9\%$ (Stramska & Stramski 2005). As more match-up data become available, more complete evaluation of the performance of POC algorithms will be possible. Another source of error in the POC_{200} is associated with the application of the mixed layer model to estimate the POC flux. This error is difficult to quantify, but the MY model simulations have been shown to compare relatively well with in situ hydrographic data and have been used to model phytoplankton dynamics within the mixed layer (e.g., Stramska et al. 1995, Ezer 2000, Zedler et al. 2002).

5. Conclusions

Quantification of regional and larger-scale estimates of POC export in the ocean from a limited number of in situ data has been a significant challenge in the past. In recent years, ocean color remote sensing has provided a powerful means for the study of ocean biogeochemistry and ecosystems over large spatial scales. Unfortunately, some quantities critical to the understanding of biogeochemical cycles and ecosystems are not directly accessible to satellite detection. We propose to examine the diffusive vertical flux of POC with a new approach that combines satellite-derived surface concentrations of POC with ocean physical models. This approach builds upon recent field-based evidence that surface POC concentrations in the ocean can be assessed directly from satellite ocean color observations (e.g., Stramski et al. 1999, Stramska & Stramski 2005). This procedure has the potential to provide long-term spatially resolved time series of diffusive POC flux, which will allow the detection of variability and trends in ocean carbon cycling. In this study, we used a one-dimensional version of the mixed layer model as a starting point, and we have shown how the seasonal and interannual variability of the diffusive component of vertical POC flux can be assessed with the use of satellite POC data as the input to the model. Because the presented approach promises significant potential for improving understanding of global POC dynamics in the ocean, more extensive numerical experiments with three-dimensional physical models are desirable in the future.

Our results provide estimates of diffusive POC flux for the example location in the north polar Atlantic. This high latitude region can be an important POC exporting system because of the occurrence of seasonal blooms and the relatively high export ratios due to the subduction of surface

waters through winter cooling and episodic deep mixing events associated with storms. Our results show that the diffusive POC flux out of the surface layer in the north polar Atlantic undergoes significant seasonal and interannual variability. The highest seasonal flux is generally observed in late fall as a result of significant convectional mixing of surface waters. A relatively high diffusive POC flux also occurs in early spring when surface waters are weakly stratified. The interannual variability of the diffusive POC flux in early spring follows the interannual pattern in the net heat loss. The highest yearly diffusive POC flux was observed in years when there was a relatively high surface POC concentration in the fall.

Although the in situ POC flux data from the time period represented by our model calculations were not available, we found that our estimates of the diffusive POC flux from the 7-year model runs lie within much the same ranges as the historical experimental POC flux data from sediment traps deployed at 200–300 m depths at the same location (Noji et al. 2000). In situ sediment trap data from a slightly different location in the north polar Atlantic and a greater depth (500 m), as well as ocean color PP models, yield only slightly higher POC export estimates in comparison to the modeled diffusive component of POC export. Notwithstanding the various sources of uncertainties in the estimates being compared, our results suggest that the diffusive component of POC flux makes a significant contribution to the total POC export in the north polar Atlantic. Atmospheric forcing is a cause of significant seasonal and interannual variability of the diffusive POC flux at the bottom of the ocean surface layer; therefore, it is also of great importance for the total POC export. In order to quantify these effects on a global scale and to understand their significance in the context of global change, similar calculations are needed with a large-scale model including 3D physics, size-dependent particle gravitational settling, and the remineralization of particles.

Acknowledgements

References

Anderson L. G., Drange H., Chierici. M, Fransson A., Johannessen T., Skjelvan I., Rey F., 2000, *Annual carbon fluxes in the upper Greenland Sea based on measurements and a box-model approach*, Tellus B, 52 (3), 1013–1024.

Antia A. N., Koeve W., Fischer G., Blanz T., Schulz-Bull D., Scholten J., Neuer S., Kremling K., Kuss J., Peinert R., Hebbeln D., Bathmann U., Conte M., Fehner U., Zeitzschel B., 2001, *Basin-wide particulate carbon flux in the Atlantic Ocean: Regional export patterns and potential for atmospheric CO_2 sequestration*, Global Biogeochem. Cy., 15 (4), 845–862.

Antoine D., Andre J.-M., Morel A., 1996, *Oceanic primary production 2. Estimation at global scale from satellite (coastal zone color scanner) chlorophyll*, Global Biogeochem. Cy., 10 (1), 57–69.

Behrenfeld M. J., Boss E., Siegel D. A., Shea D. M., 2005, *Carbon-based ocean productivity and phytoplankton physiology from space*, Global Biogeochem. Cy., 19 (1), GB1006, doi:10.1029/2004GB002299.

Behrenfeld M. J., Falkowski P. G., 1997, *Photosynthetic rates derived from satellite-based chlorophyll concentration*, Limnol. Oceanogr., 42 (1), 1–20.

Berelson W., 2001, *The flux of particulate organic carbon into the ocean interior: A comparison of four JGOFS regional studies*, Oceanography, 14 (4), 59–67.

Berger W. H., Fischer K., Lai C., Wu G., 1987, *Ocean carbon flux: Global maps of primary production and export production*, [in:] *Biogeochemical cycling and fluxes between the deep euphotic zone and other oceanic realms*, C. Agegian (ed.), SIO Ref. 87–30, Univ Calif., San Diego; Scripps Inst. Oceanogr., La Jolla, California, 44 pp.,

Betzer P. R., Showers W. J., Laws E. A., Winn C. D., DiTullio G. R., Kroopnik P. M., 1984, *Primary productivity and particle fluxes on a transect of the equator at 153° W in the Pacific Ocean*, Deep-Sea Res. Pt. A, 31, 1–11.

Blumberg A. F., Mellor G. L., 1983, *Diagnostic and prognostic numerical circulation studies of the South California Bight*, J. Geophys. Res., 88, 4579–4592.

Boyd P. W., Stevens C. L., 2002, *Modelling particle transformations and the downward organic carbon flux in the NE Atlantic Ocean*, Prog. Oceanogr., 52 (1), 1–29.

Buesseler K. O., Andrews J. A., Hartman M. C., Belastock R., Chai F., 1995, *Regional estimates of the export flux of particulate organic carbon derived from ^{234}Th during the JGOFS EqPac program*, Deep-Sea Res. Pt. II, 42 (2–3), 777 –804.

Buesseler K. O., Bacon M. P., Cochran J. K., Livingston H. D., 1992, *Carbon and nitrogen export during the JGOFS North Atlantic bloom experiment estimated from ^{234}Th: ^{238}U disequilibria*, Deep-Sea Res., 39, 1115–1137.

Druet C., 2003, *The fine structure of marine hydrophysical fields and its influence on the behaviour of plankton: an overview of some experimental and theoretical investigations*, Oceanologia, 45 (4), 517–555.

Druet C., Zielinski A., 1994, *Modelling the fine-structure of the phytoplankton concentration in a stable stratified sea*, Oceanol. Acta, 17, 79–88.

Ducklow H. W., Steinberg D. K., Buesseler K. O., 2001, *Upper ocean carbon export and the biological pump*, Oceanography, 14 (4), 50–58.

Dugdale R. C., Goering J. J., 1967, *Uptake of new and regenerated forms of nitrogen in primary productivity*, Limnol. Oceanogr., 12, 196–206.

Dzierzbicka-Głowacka L., 2005a, *Modelling the seasonal dynamics of marine plankton in southern Baltic Sea. Part 1. A coupled ecosystem model*, Oceanologia, 47 (4), 591–619.

Dzierzbicka-Głowacka L., 2005b, *Modelling the seasonal dynamics of marine plankton in southern Baltic Sea. Part 2. Numerical simulations*, Oceanologia, 48 (1), 41–71.

Eppley R. W., 1989, *New production, history, methods, problems*, [in:] *Productivity of the ocean: Present and past*, W. H. Berger, V. S. Smetacek & G. Wefer (eds.), Wiley & Sons, New York.

Eppley R. W., Petersen B. J., 1979, *Particulate organic matter flux and planktonic new production in the deep ocean*, Nature, 282 (5754), 677–680.

Ezer T., 2000, *On the seasonal mixed layer simulated by a basin-scale ocean model and the Mellor-Yamada turbulence scheme*, J. Geophys. Res., 105 (C7), 16843 –16855.

Fasham M. J. R., Ducklow H. W., McKelvie S. M., 1990, *A nitrogen-based model of plankton dynamics in the oceanic mixed layer*, J. Mar. Res., 48, 591–639.

Gordon H. R., Wang M., 1994, *Retrieval of water-leaving radiance and aerosol optical thickness over the oceans with SeaWiFS: A preliminary algorithm*, Appl. Opt., 33, 443–452.

Hooker S. B., McClain C. R., 2000, *The calibration and validation of SeaWiFS data*, Prog. Oceanogr., 45 (3–4), 427–465.

Huisman J., van Oostveen P., Weissing F. J., 1999, *Critical depth and critical turbulence: two different mechanisms for the development of phytoplankton blooms*, Limnol. Oceanogr., 44 (7), 1781–1788.

Jerlov N. G., 1968, *Optical oceanography*, Elsevier, New York, 194 pp.

Laws E. A., Falkowski P. G., Smith W. O., Ducklow H., McCarthy J. J., 2000, *Temperature effects on export production in the open ocean*, Global Biogeochem. Cy., 14 (4), 1231–1246.

Legendre L., Rivkin R. B., 2002, *Fluxes of carbon in the upper ocean: Regulation by food-web control nodes*, Mar. Ecol. Prog. Ser., 242, 95–109.

Lima I. D., Doney S. C., 2004, *A three-dimensional, multinutrient, and size-structured ecosystem model for the North Atlantic*, Global Biogeochem. Cy., 18 (3), GB3019, doi:10.1029/2003GB002146.

Lutz M., Dunbar R., Caldeira K., 2002, *Regional variability in the vertical flux of particulate organic carbon in the ocean interior*, Global Biogeochem. Cy., 16 (3), 1037, doi:10.1029/2000GB001383.

Marra J., Ho C., 1993, *Initiation of the spring bloom in the northeast Atlantic (47°N, 20°W): A numerical simulation*, Deep-Sea Res. Pt. II, 40 (1–2), 55–73.

Martin J. H., Fitzwater S. E., Gordon R. M., Hunter C. N., Tanner S., 1993, *Iron, primary production, and carbon-nitrogen flux studies during the JGOFS North Atlantic Bloom Experiment*, Deep-Sea Res. Pt. II, 40 (1–2), 115–134.

Martin J., Knauer G., Karl D., Broenkow W., 1987, *VERTEX: carbon cycling in the northeast Pacific*, Deep-Sea Res., 34, 267–286.

Mellor G. L., Yamada T., 1974, *A hierarchy of turbulence closure models for planetary boundary layers*, J. Atmos. Sci., 31, 1791–1806.

Mellor G. L., Yamada T., 1982, *Development of a turbulence closure model for geophysical problems*, Rev. Geophys. Space Phys., 20, 851–857.

Mellor G. L, 2004, *Users Guide for a three-dimensional, primitive equation numerical ocean model*, Available on the Princeton Ocean Model (POM) web site, rev. 2004, (http://www.aos.princetion.edu/WWPUBLIC/htdocs.pom/).

Noji T. T., Miller L. A., Skjelvan I., Falck E., Borsheim K. Y., Rey F., Urban-Rich J., Johannessen T., 2000, *Constraints on carbon drawdown and export in the Greenland Sea*, [in:] *The Northern North Atlantic: A changing environment*, P. Schafer, W. Ritzrau, M. Schluter & J. Thiede (eds.), Springer, Berlin, 39–52.

Pace M. L., Knauer G. A., Karl D. M., Martin J. H., 1987, *Primary production, new production and vertical flux in the eastern Pacific Ocean*, Nature, 325 (6107), 803–804.

Paulson C. A., Simpson J. J., 1977, *Irradiance measurements in the upper ocean*, J. Phys. Oceanogr., 7, 952–956.

Pätsch J., Kühn W., Radch G., Santana Casiano J. M., Gonzalez Davila M., Neuer S., Freudenthal T., Llinas O., 2002, *Interannual variability of carbon fluxes at the North Atlantic Station ESTOC*, Deep-Sea Res. Pt. II, 49 (1–3), 253–288.

Schlitzer R., 2002, *Carbon export fluxes in the Southern Ocean: results from inverse modeling and comparison with satellite-based estimates*, Deep-Sea Res. Pt. II, 49 (9–10), 1623–1644.

Schlitzer R., 2004, *Export production in the Equatorial and North Pacific derived from dissolved oxygen, nutrient and carbon data*, J. Oceanogr., 60 (1), 53–62.

Schlitzer R., Usbeck R., Fischer G., 2003, *Inverse modeling of particulate organic carbon fluxes in the South Atlantic*, [in:] *The South Atlantic in the late quaternary: reconstruction of material budgets and current systems*, Springer-Verlag, Berlin; Heidelberg; New York; Tokyo, 1–19.

Siegel D. A, Deuser W. G., 1997, *Trajectories of sinking particles in the Sargasso Sea: Modeling of statistical funnels above deep-ocean sediment traps*, Deep-Sea Res. Pt. I, 44 (9–10), 1519–1541.

Stramska M., Dickey T. D., Marra J., Plueddemann A., Langdon C., Weller R., 1995, *Bio-optical variability associated with phytoplankton dynamics in the North Atlantic Ocean during spring and summer of 1991*, J. Geophys. Res., 100 (C4), 6621–6632.

Stramska M., Stramski D., 2005, *Variability of particulate organic carbon concentration in the north polar Atlantic based on SeaWiFS ocean color observations*, J. Geophys. Res., 110 (C10018), doi:10.1029/2004JC002762.

Stramski D., Reynolds R. A., Kahru M., Mitchell B. G., 1999, *Estimation of particulate organic carbon in the ocean from satellite remote sensing*, Science, 285 (5425), 239–242.

Suess E., 1980, *Particulate organic carbon flux in the oceans – surface productivity and oxygen utilization*, Nature, 288 (5788), 260–263.

Usbeck R., Schlitzer R., Fischer G., Wefer G., 2003, *Particle fluxes in the ocean: Comparison of sediment trap data with results from inverse modeling*, J. Marine Syst., 39 (3–4), 167–182.

von Bodungen B., Antia A., Bauerfeind E., Haupt O., Koeve W., Machado E., Peeken I., Peinert T., Reitmeier S., Thomsen C., Voss M., Wunsch M., Zeller U., Zeitzschel B., 1995, *Pelagic processes and vertical flux of particles: an overview of a long-term comparative study in the Norwegian Sea and Greenland Sea*, Geol. Runds., 84 (1), 11–27.

Westberry T. K., Behrenfeld M. J., Boss E., Siegel D. A., 2006, *Carbon-based net primary production and phytoplankton growth rates from ocean color measurements: Part II*, Ocean Sciences Meeting, Honolulu, February 20–24, 2006.

Zedler S. E., Dickey T. D., Doney S. C., Price J. F., Yu X., Mellor G. L., 2002, *Analysis and simulations of the upper ocean's response to Hurricane Felix at the Bermuda Testbed Mooring site: August 13–23, 1995*, J. Geophys. Res., 107(C12), 3232, doi:10.1029/2001JC000969.